

Geophysical Research Letters[®]

RESEARCH LETTER

10.1029/2022GL098077

Special Section:

Results from Juno's Flyby of Ganymede

Key Points:

- We present energy spectra from energetic charged particle data from Juno's close flyby of Ganymede in 2021
- We find a drop in electron fluxes on polar field lines compared to the surrounding region whereas ion fluxes are similar in both regions
- We compute sputtering rates to evaluate particle weathering, as a step toward understanding the distribution of Ganymede's surface ice

Correspondence to:

C. Paranicas,
chris.paranicas@jhuapl.edu









Citation:

Paranicas, C., Mauk, B. H., Kollmann, P., Clark, G., Haggerty, D. K., Westlake, J., et al. (2022). Energetic charged particle fluxes relevant to Ganymede's polar region. *Geophysical Research Letters*, 49, e2022GL098077. <https://doi.org/10.1029/2022GL098077>

Received 31 JAN 2022
Accepted 7 MAY 2022

© 2022 The John Hopkins University Applied Physics Lab. This is an open access article under the terms of the [Creative Commons Attribution-NonCommercial License](https://creativecommons.org/licenses/by-nc/4.0/), which permits use, distribution and reproduction in any medium, provided the original work is properly cited and is not used for commercial purposes.

Energetic Charged Particle Fluxes Relevant to Ganymede's Polar Region

C. Paranicas¹ , B. H. Mauk¹ , P. Kollmann¹ , G. Clark¹ , D. K. Haggerty¹ , J. Westlake¹ , L. Liuzzo² , A. Masters³ , T. A. Cassidy⁴, F. Bagenal⁴ , and S. Bolton⁵ 

¹APL, Laurel, MD, USA, ²Space Sciences Lab, University of California, Berkeley, CA, USA, ³Blackett Laboratory, Imperial College, London, UK, ⁴University of Colorado, Boulder, CO, USA, ⁵SWRI, San Antonio, TX, USA

Abstract The JEDI instrument made measurements of energetic charged particles near Ganymede during a close encounter with that moon. Here we find ion flux levels are similar close to Ganymede itself but outside its magnetosphere and on near wake and open field lines. But energetic electron flux levels are more than a factor of 2 lower on polar and near-wake field lines than on nearby Jovian field lines at all energies reported here. Flux levels are relevant to the weathering of the surface, particularly processes that affect the distribution of ice, since surface brightness has been linked to the open-closed field line boundary. For this reason, we estimate the sputtering rates expected in the polar regions due to energetic heavy ions. Other rates, such as those related to radiolysis by plasma and particles that can reach the surface, need to be added to complete the picture of charged particle weathering.

Plain Language Summary This paper uses Juno data to quantify the levels of energetic charged particle flux near Jupiter's moon Ganymede. We have computed energy spectra (energy vs. charged particle intensity) for electrons, protons, oxygen and sulfur ions, from a near encounter of Ganymede by the Juno spacecraft in June 2021. Particle fluxes may be important for weathering processes on Ganymede, such as the sputtering of water ice in the top layer. The distribution of water ice in the upper layer of Ganymede's surface does not appear to be consistent with sublimation alone, so questions remain about which processes are dominant in shaping the ice distribution. Quantification of the flux levels is also needed for planning, for example, for ESA's JUICE mission, expected to orbit Ganymede in the future.

1. Introduction

On 7 June 2021, the Juno spacecraft had its closest flyby of Jupiter's moon Ganymede to date, at an altitude of about 1,046 km. The radius of the moon is 2,634 km. The closest approach occurred over the leading hemisphere of the moon, that is, in the plasma wake region. The spacecraft accessed “open” magnetic field lines of Ganymede, that is, those connected to both Jupiter and Ganymede. The detailed geometry of the flyby can be found in Clark et al. (2022).

In this paper, we will focus on data obtained by the Jupiter Energetic particle Detector Instrument (JEDI) during that flyby. The instrument has been fully described in Mauk et al. (2017). The main channels of interest here are the tens of keV to nearly 1 MeV electron channels and the time-of-flight by energy channels, which can separately detect protons (from the tens of keV to 1 MeV), and oxygen and sulfur ions (from the hundreds of keV to 10 MeV energies).

The last spacecraft to make close flybys of Ganymede was Galileo. Williams et al. (1998), for example, presented data from the Energetic Particles Detector (EPD), which covers a similar energy range as JEDI, during several Ganymede flybys. In that paper, they displayed the count rate versus time for one total ion channel and two electron channels. They found the fluxes of tens to hundreds of keV electrons were generally lower on polar field lines than in the surrounding medium. Electron fluxes dropped dramatically in the large loss cone created by Ganymede but, even outside the loss cone, flux levels were still lower on open field lines than on nearby Jovian field lines (i.e., both ends on Jupiter). Total ion fluxes did not decrease much from the ambient environment to the polar region, except within the loss cone. But from the total ion count rate, for example, in their Figure 2, it can be inferred that the plasma flow speed over Ganymede's poles was much slower than on Jovian field lines. This is apparent in the amplitude of the sine wave pattern in the count rate when it is plotted versus time, due to the Compton-Getting effect (e.g., Gleeson & Axford, 1968). In this paper, we will present much more detailed

information about the region near Ganymede, including quantitative information about the energy spectra for four species (electrons, protons, oxygen and sulfur ions). Characterizing these levels is important for several reasons including as inputs to models of the effects of the environment on the surface and satellite atmosphere and for planning for future missions to the Jovian system.

While it is still unknown how much particle weathering explains Ganymede's surface features, there are indications that it is an important process. Ligier et al. (2019) have pointed out, using ground-based data, that in abundance maps of water ice, the equatorial latitudes of Ganymede contain less water ice than the polar regions, in the top layer of the surface. With their infrared data, they were only able to probe the surface to a relatively shallow depth. While this polar versus equatorial pattern is qualitatively consistent with sublimation, the complete answer is probably more complicated. For example, among equatorial latitudes only, Ligier et al. (2019) also found that the trailing apex region has the smallest amount of water ice on the surface.

Plainaki et al. (2020) recently simulated how particles would impact Ganymede's surface. That work considers the polar/equatorial albedo dichotomy from a weathering point of view and also suggests how weathering and sublimation can maintain darker surface regions. But they do not provide a mechanism for the original cause of the feature centered on the trailing apex nor, like many recent simulations, attempt to exactly match the latitude-longitude dimensions of the feature (Ligier et al., 2019) with the ion precipitation patterns they derive.

If Ganymede were not magnetized, the trailing apex feature might be consistent with direct sputtering of the ice by magnetospheric plasma and particles. This is because these particles overtake Ganymede in its orbit and preferentially impact the trailing hemisphere. Previously, Paranicas et al. (2021) put forward the hypothesis that if ions charge-exchange near Ganymede, they can hit the surface as energetic neutral atoms (ENAs) and sputter the ice. ENAs from ions approaching Ganymede would essentially inherit the ion's final velocity vector which has a contribution from the plasma flow. In addition, Europa and Callisto have compositional changes centered on their trailing apex points. An oxygen ion would get converted to an ENA with a probability $\sim 10^{-4}$ if it passed close to Ganymede, using a hydrogen density at high altitude from Marconi (2007), a charge-exchange cross-section of a $\sim 5 \times 10^{-16}$ cm² (e.g., Paranicas et al., 2008) and a path length of Ganymede's diameter. There is no question then that ENAs will be formed near Ganymede and the energetic, heavy ENAs will sputter the ice with a high yield. The question is whether the surface erosion rate of such a process would be competitive with other surface modification processes and this question requires a more rigorous quantitative analysis. In addition, it is likely the distribution of surface ice is shaped by many factors and the external driving environment may have a complex role.

1.1. Overview of the Energetic Charged Particle Data

In Figure 1, we show an overview of the JEDI electron and proton intensities measured during the Juno Ganymede encounter on day 2021-158. Clark et al. (2022) have created a complementary figure displaying integrated intensity versus local pitch angle. They have proposed that the time between 16:45:30 and 17:00:30 contains evidence of the main particle losses in the JEDI data. We have indicated in Figure 1 our preliminary view of whether Juno was in the wake or on open field lines during that time interval. During that time, the electron intensity at all JEDI energies shows a decrease. This is broadly consistent with predictions made by Liuzzo et al. (2020). They suggested that energetic electron flux over the polar trailing hemisphere regions would be similar to the upstream region but after precipitation, enhanced by the flow reduction, the flux above Ganymede's polar leading hemisphere would be slightly reduced compared to the ambient population.

As we discuss further below, the proton data do show a transition from the purely Jovian field lines to those affected by Ganymede, but it is less pronounced than in the electron data. The work of Jia et al. (2008), for example, their Figure 6, suggests that the boundary between Jovian and polar Ganymede field lines would not, by itself, limit the access of large gyroradius particles. A 1 MeV electron has a gyroradius of ~ 37 km compared to $\sim 4,479$ km for 1 MeV O⁺ in a magnetic field with values typical of Ganymede's orbital distance. The field configurations derived in Jia's work provide clues to the organization of the JEDI data.

Figure 1 is also broadly consistent with the Energetic Particles Detector (EPD) data shown in Williams et al. (1998). The fluxes of approximately 50 keV to 1 MeV electrons show a decrease (compared with those on Jovian field lines) that persists over Ganymede's poles. On the other hand, the proton fluxes at all energies presented show almost no change when Juno first moves from Jovian field lines into the wake, but there is a

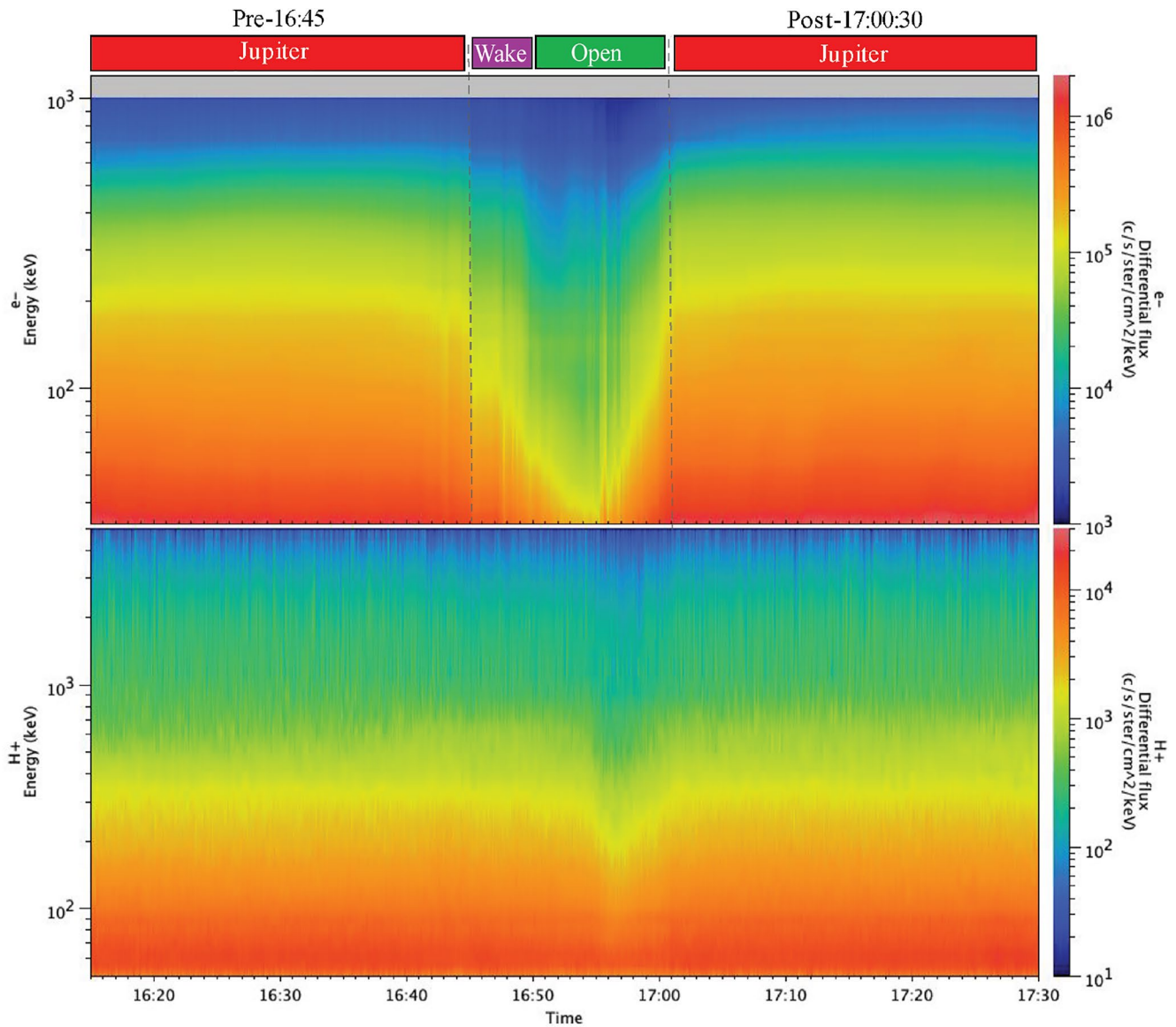


Figure 1. Electron (top) and proton (bottom) intensities in the approximately 75 min around Juno's close approach to Ganymede. The top panel has a standard electron correction applied to the data and combines all 3 Jupiter Energetic particle Detector Instruments and all local pitch angles. The bottom panel combines data from JEDI-90 and JEDI-270 and all local pitch angles. The likely locations of the wake and open field line regions are indicated and we refer to them collectively in the text just as, "polar".

decrease in flux on a portion of the polar field lines several minutes later. Most of these polar field lines map to Ganymede's leading hemisphere.

1.2. Energy Spectra

In Figure 2, we display electron energy spectra from JEDI data. For each species for which we compute energy spectra in this paper, we average data from approximately 16:45 to 17:00 UT and also on Jovian field lines that are well away from the boundaries using the time periods: 16:10–16:30 and 17:10–17:30 UT. The data used for spectra include charged particles whose local pitch angles are between 30° and 150° . These data have been corrected but we also show, for illustrative purposes only, uncorrected data from the open field lines (circles). The change in slope among the black circles that begins at about 100 keV is due to roughly 1 MeV or greater electrons that fully penetrate the detector. They leave a fraction of their energy in the JEDI SSDs, which mimics the energy loss

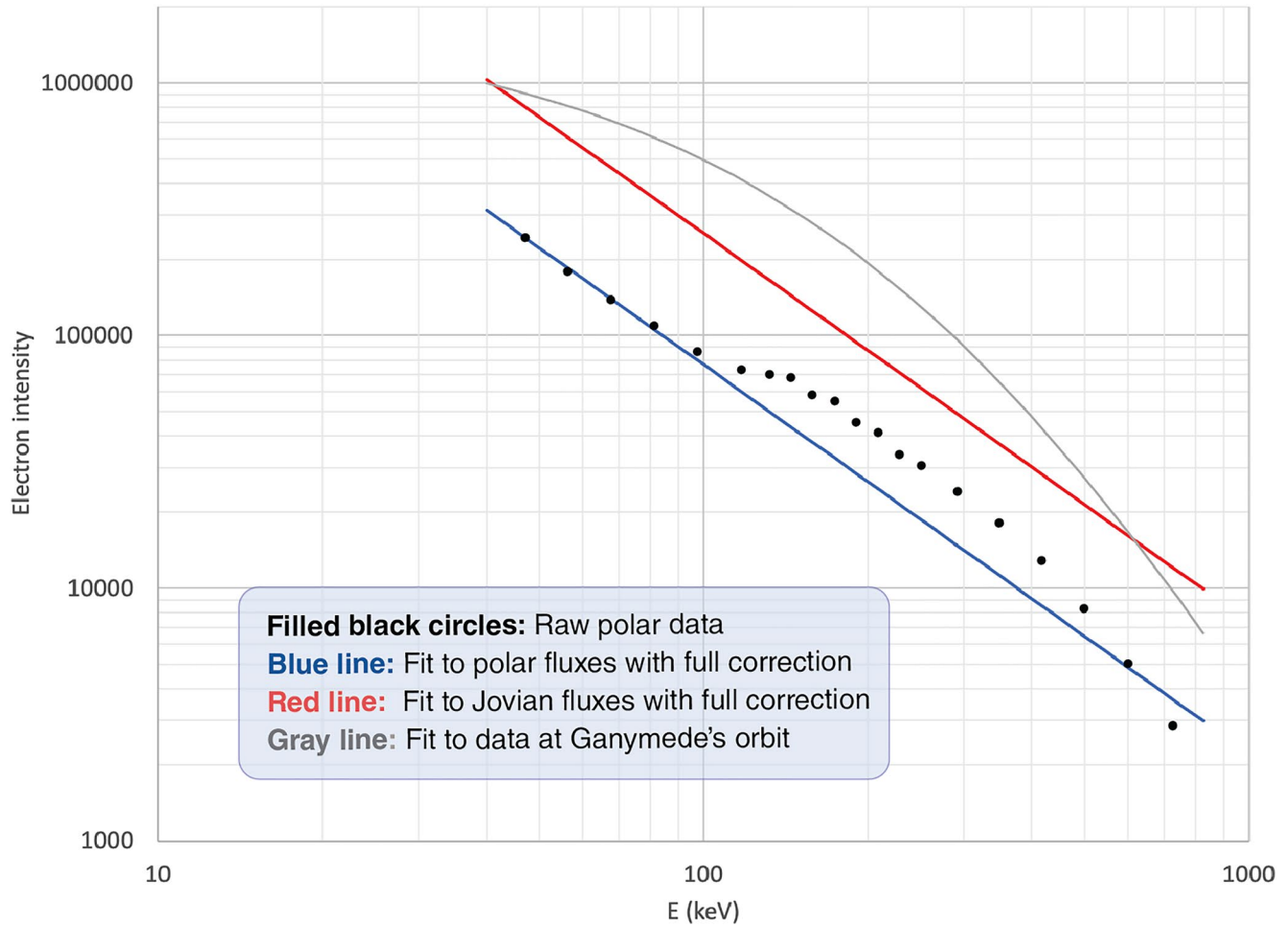


Figure 2. Electron intensities (electrons per $\text{cm}^2\text{-s-sr-keV}$) from Jupiter Energetic particle Detector Instrument (JEDI) data. The black dots show uncorrected JEDI data obtained on Jupiter-Ganymede field lines. Two lines show a quantitative fit to the data from the encounter on polar (blue) and Jovian (red) field lines. The gray curve shows a fit to the electron data (Paranicas et al., 2021) obtained at Ganymede's orbital distance far from the moon.

expected for 100–200 keV electrons. Furthermore, the count rate of the inferred population of >1 MeV electrons (not shown) also decreases on polar field lines by a factor of 2 or so. We include a fit to data obtained on 2019-148 17:00–17:20 (Paranicas et al., 2021). During that time period, Juno was near the magnetic equator at Ganymede's orbital distance, but longitudinally very far from it.

In Paranicas et al. (2021), we used the standard correction to the electron data to account for the loss of efficiency at high energy on JEDI (near the top end of its energy range) and for particles that deposit energy into the detectors around and mostly above 160 keV but are actually higher energy particles that have completely passed through the detectors and did not leave all of their energy behind. This is the same correction that was applied to the electron data shown in Figure 1. But in Figure 2, we performed a more rigorous version of the correction focusing on the same two issues. The supplemental material in Mauk et al. (2018) outlines a procedure for recovering the charged particle intensity, j in counts per $\text{cm}^2\text{-s-sr-keV}$, as a function of energy (E), modeled as,

$$j = CE \frac{[E + kT(g1 + 1)]^{-g1-1}}{1 + \left(\frac{E}{E_0}\right)^{g2}}$$

where E , E_0 , and kT are all in keV, and the fit parameters (C , kT , E_0 , $g1$, and $g2$) are listed in Table 1. The circles and the blue line in the figure illustrate how this correction procedure alters the raw data. When the corrected JEDI data are compared to an intensity from Galileo Energetic Particles Detector (EPD) taken a number

Table 1
Parameters for the Electron Intensity Fit by Region

	Jupiter	Polar
C	8.3e + 08	4.1e + 08
kT	0.03	0.03
g1	0.74	0.72
E_o	0.29	0.166
g2	0.80	0.82

of Ganymede radii from the moon, the value at 100 keV from Figure 2 of Paranicas et al. (1999) is a factor of 10 lower than the value for the Jovian flux here. A thorough analysis of the variability of the energetic electron population from the Juno data can be found in Ma et al. (2021).

In Figure 3, we show proton energy spectra from Ganymede's near wake and open field line region and from Jovian field lines near Ganymede. Again, we show a fit to proton data (black line) obtained at Ganymede's orbital distance but not near the moon, from Paranicas et al. (2021). It can be seen that the proton intensities at these energies are similar on open field lines and in the regions surrounding Ganymede's magnetosphere. There is some departure at a range of energies between the 2021 data and the fit to the data upstream and

well away from Ganymede. But two energy spectra computed from data even taken at the exact same position in the magnetosphere can be different because of time variations in the environment itself and, for example, by how local pitch angles are sampled each time and treated in the averages, if the pitch angle distribution is not isotropic.

In Figure 4, we show oxygen and sulfur energy spectra from Jovian field lines near Ganymede during this encounter and from data obtained on polar Ganymede field lines. These levels are about the same in the two species at

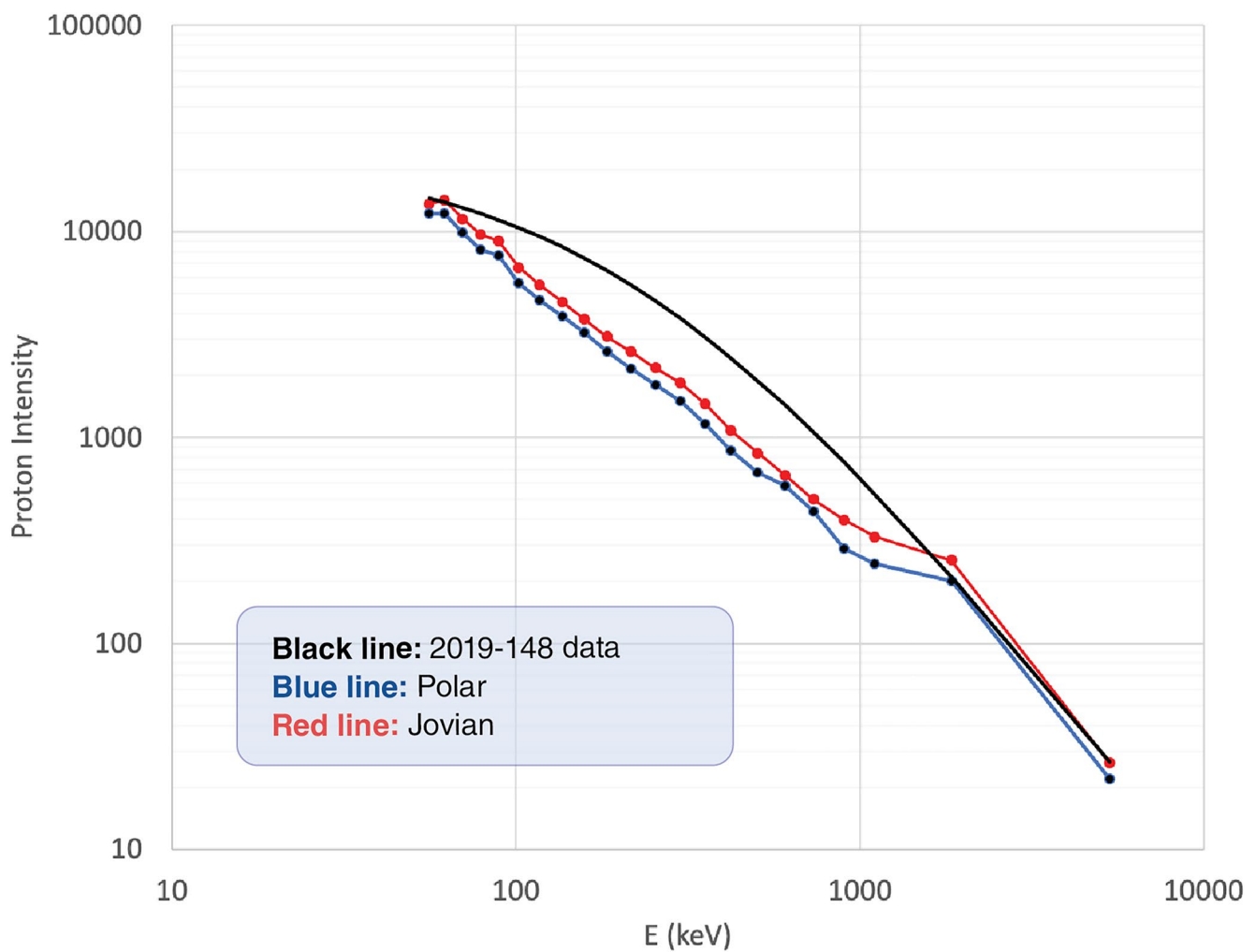


Figure 3. Proton intensity from Jupiter Energetic particle Detector Instrument showing data from the polar (blue) and Jovian (red) field lines. Overplotted is a fit to the proton data (black) from Paranicas et al. (2021), which used data from 2019-148 17:00-17:20 UT.

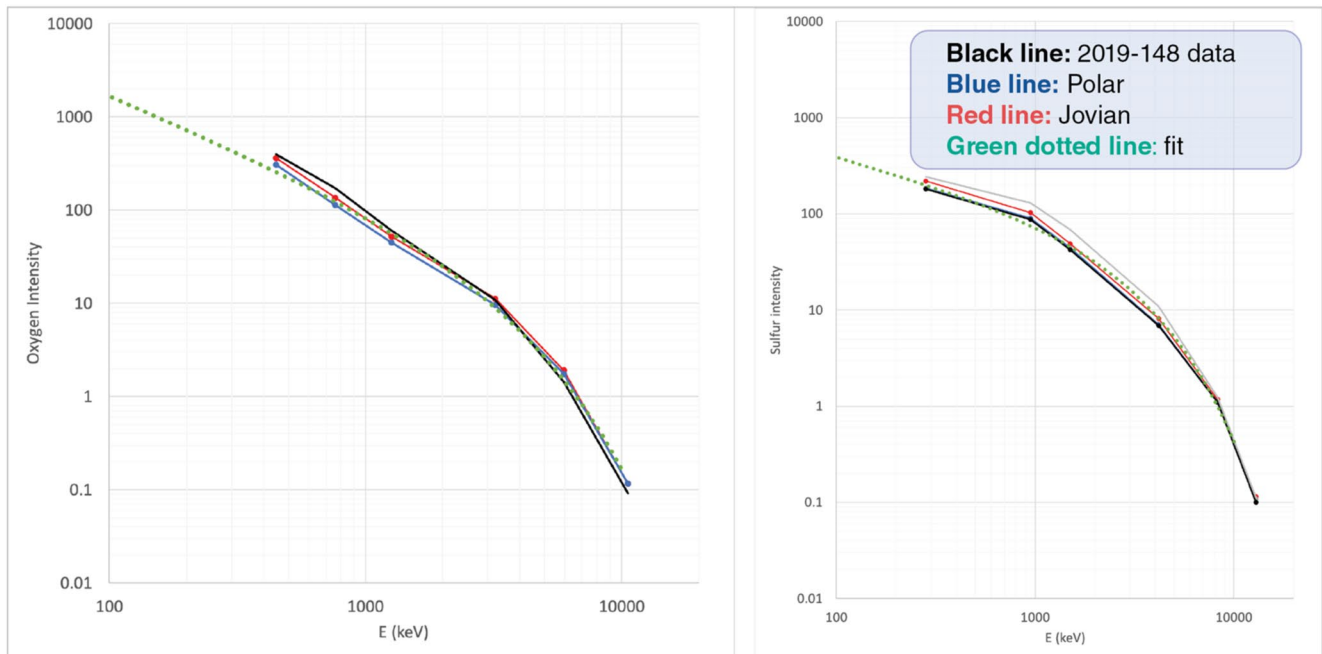


Figure 4. Oxygen and sulfur intensities from Jupiter Energetic particle Detector Instrument. The curves are from polar (blue) and Jovian (red) field lines for both oxygen and sulfur. The black curves are data from the time period 2019-148 17:00–17:20 UT when Juno was at Ganymede's orbital distance but far away from the moon. The green dashed line is a fit function, $j = j_{\text{species}} \times E^{-a} \times \exp(-E/E_{\text{species}})$, with all energies in keV. For oxygen, $J_{\text{ox}} = 3.5 \times 10^5$, $E_{\text{ox}} = 2,550$, $a = -1.15$, and for sulfur, $J_{\text{su}} = 5.7 \times 10^3$, $E_{\text{su}} = 2,382$, $a = -0.57$.

1 MeV but oxygen fluxes are trending higher at lower energy. We also show a fit to the data obtained on polar field lines (green dotted line). Since the flow over the poles is slow, these fits can be thought of as approximating the flux in the plasma rest frame. We have added data from day 2019-148 between 17:00–17:20 UT (black curves), a time period when Juno crossed Jupiter's magnetic equator at Ganymede's orbital distance that we considered in an earlier work. The levels by region are all very similar, with a few energies showing a difference of up to a factor of 2 between the data near Ganymede and over its poles. Finally, given that the energy channel coverage of heavy ions is coarser than protons on JEDI, we do not present spectrograms of those data, but the curves in Figure 4 indicate that the decrease is more like the protons than the electrons.

For the limited amount of ion data presented here, the values on polar (and mainly leading hemisphere) and nearby Jovian field lines are similar, but flux levels may vary considerably at different Ganymede altitudes and longitudes for other reasons (e.g., Kollmann et al., 2022). As noted, this is consistent with the single total ion channel presented in Williams et al. (1998). It is also similar to some of the environmental modeling. For example, Plainaki et al. (2015) found that the fluxes of 100 keV oxygen ions were somewhat uniform in a wide region around Ganymede. It was only on closed Ganymede field lines that they found important flux differences. Likewise, Plainaki et al. (2020), their Figures 2 and 4, also found proton and oxygen fluxes similar in the upstream/ambient and polar regions, although for energies slightly below the energy range of JEDI measurements.

2. Discussion

The JEDI data presented here reveal that the largest charged particle flux differences among the regions near Ganymede are in energetic electrons. This is probably due to the bounce period of ions versus electrons. As particles drift across Ganymede's polar caps in their circumplanetary motion, electrons are more likely to be lost at the moon's surface than ions of the same energy. Williams et al. (1998) showed that the loss cone created by Ganymede is large. Electrons bounce much faster than ions of the same energy between the moon and the planet (roughly seconds vs. minutes). Therefore, electrons will have a higher probability of being lost at Ganymede. In

this picture, losses are expected to be enhanced for all species by the slower plasma flow speed over the poles and scattering into the loss cone.

If the greater reduction of electrons than ions over the poles is due to the Ganymede loss cone, it is the difference in gyroradius that helps to ensure the levels are kept separated on the two field line topologies. Charged particles have a gyroradius about the same size as the moon's radius for energies as follows: 101.4 MeV electrons, 5.52 MeV protons, 0.346 MeV O⁺, and 0.173 MeV S⁺, assuming an equatorial magnetic field strength of 0.00127 G (=4.28/15³ Gauss) and particles with mirror latitudes of 5° in a dipole field. These values suggest ions can move between the open and Jovian field lines more easily during their gyromotion.

Particle fluxes, by level and location around the moon, are important for understanding whether charged particles can play a role in the appearance of Ganymede's surface ice. Overall, the poles are brighter than the equator in the visible and, within the equatorial region, the leading hemisphere is brighter than the trailing one (Pappalardo et al., 2004). These features correlate with where the water ice is most abundant in the very top layer of the surface (Ligier et al., 2019). This suggests to us that processes that mobilize, redistribute, or alter the water ice, such as sublimation, radiolysis (e.g., Plainaki et al., 2020; Teolis et al., 2017), sputtering (e.g., Famá et al., 2008; Galli et al., 2018), and dust and other impacts, are likely important for the albedo. Processes that darken the ice (e.g., Hand & Carlson, 2015; Hedman et al., 2020) might be secondary at Ganymede.

A key driver of the polar versus equatorial distribution may be sublimation (Ligier et al., 2019; Marconi, 2007; Roth et al., 2021). But sublimation alone is unlikely to provide the full answer. It does not explain the albedo difference across the open-closed boundary (Khurana et al., 2007) or the longitudinal differences in the equatorial region (Ligier et al., 2019). It is more likely that sublimation plus another process drives the ice distribution in the top layer of Ganymede's surface.

The energy spectra presented in this paper are useful for computing partial moments of the distribution function, especially since the flow is very slow over the poles, meaning the functions on polar field lines are basically in the rest frame of the plasma. These energy spectra are also useful for predicting ion sputtering rates taking into consideration energy-dependent sputtering yield functions (e.g., Galli et al., 2018; Teolis et al., 2017). An early view of Ganymede's bright polar caps was that the ice was sputtered over the whole surface but was more like to recondense at the cold poles, resulting in a brighter appearance there (Johnson, 1985; Sieveka & Johnson, 1982). But newer work has suggested that other plasma and particle weathering processes are important (e.g., Carnielli et al., 2020; Davis et al., 2021; Plainaki et al., 2020; Teolis et al., 2017). For example, Davis et al. (2021) argued that at Europa electrons play a more important role in the erosion of water ice than ions.

If the Jupiter-Ganymede field line fluxes detected by Juno are taken to be a reasonable approximation to the precipitation fluxes, we compute the sputtering rates to be: 4.5×10^8 per cm²-s for oxygen and 1.4×10^9 per cm²-s for sulfur, assuming the target is pure water ice. For these values, we have integrated from about 100 keV to 10 MeV only, used the sputtering yield function provided by Johnson et al. (2004), and only consider the polar region. Plainaki et al. (2020) estimated the sputtering rate over the whole surface as, 2.6×10^{26} per s. Another good discussion of the drivers of sputtering is provided by Cassidy et al. (2013) for Europa.

In summary, the JEDI data have been used to compare fluxes of energetic charged particles near Ganymede's orbit, near the moon itself, and on Jupiter-Ganymede field lines. Among energetic charged particles, only electron fluxes are reduced at all measured energies between the polar field lines and nearby Jovian ones. If we ignore how particles get into the loss cone created by Ganymede, this suggests that polar surface weathering processes can be crudely approximated using fluxes in the surrounding space. To make all the observational data on albedo fit together, the process of sublimation is not sufficient. Therefore, if weathering by plasma and particles play a dominant role in the distribution of the ice and the brightness of Ganymede, more work is needed on the various pathways from environment to surface, for example, in connecting the simulations to the exact patterns of water ice distribution reported by Ligier et al. (2019).

Data Availability Statement

The Planetary Data System provides access to the Juno JEDI data, <https://pds-ppi.igpp.ucla.edu/search/?sc=Juno&t=Jupiter&i=JEDI>.

Acknowledgments

The first author would like to thank J. E. P. Connerney for supplying magnetic field measurements at a high cadence that allows JEDI to associate magnetic pitch angles to the data and James Peachey for maintaining the analysis software used for this project. CP also appreciates insights by both referees and discussions with C. Plainaki, M. Hedman, and A. Hendrix. AM is supported by a Royal Society University Research Fellowship. This work was funded by the Juno project through contracts between JHU/APL and SWRI.

References

Carnielli, G., Galand, M., Leblanc, F., Modolo, R., Beth, A., & Jia, X. (2020). Simulations of ion sputtering at Ganymede. *Icarus*, 351. <https://doi.org/10.1016/j.icarus.2020.113918>

Cassidy, T. A., Paranicas, C., Shirley, J., Dalton, J., III, Teolis, B., Johnson, R., et al. (2013). Magnetospheric ion sputtering and water ice grain size at Europa. *Planetary and Space Science*, 77, 64–73. <https://doi.org/10.1016/j.pss.2012.07.008>

Clark, G., Kollmann, P., Mauk, B., Paranicas, C., Haggerty, D., Rymer, A., et al. (2022). Energetic charged particle observations during Juno's close flyby of Ganymede. *Geophysical Research Letters*, 49, e2022GL098572. <https://doi.org/10.1029/2022GL098572>

Davis, M. R., Meier, R. M., Cooper, J. F., & Loeffler, M. J. (2021). The contribution of electrons to the sputter-produced O₂ exosphere of Europa. *The Astrophysical Journal Letters*, 908(2), L53. <https://doi.org/10.3847/2041-8213/abe415>

Famá, M., Shi, J., & Baragiola, R. A. (2008). Sputtering of low-energy ions. *Surface Science*, 602(1), 156–161. <https://doi.org/10.1016/j.susc.2007.10.002>

Galli, A., Vorbürger, A., Wurz, P., Cerubini, R., & Tulej, M. (2018). First experimental data of sulphur ions sputtering water ice. *Icarus*, 312, 1–6. <https://doi.org/10.1016/j.icarus.2018.04.029>

Gleeson, L. J., & Axford, W. I. (1968). The Compton-Getting effect. *Astrophysics and Space Science*, 2(4), 431–437. <https://doi.org/10.1007/bf02175919>

Hand, K. P., & Carlson, R. W. (2015). Europa's surface color suggests an ocean rich with sodium chloride. *Geophysical Research Letters*, 42(9), 3174–3178. <https://doi.org/10.1002/2015gl063559>

Hedman, M. M., Helfenstein, P., Chancia, R. O., Thomas, P., Roussos, E., Paranicas, C., & Verbiscer, A. J. (2020). Photometric analysis of Saturn's small moons: Aegaeon, Methone, and Pallene are dark; Helene and Calypso are bright. *The Astronomical Journal*, 151. <https://doi.org/10.3847/1538-3881/ab659d>

Jia, X., Walker, R. J., Kivelson, M. G., Khurana, K. K., & Linker, J. A. (2008). Three-dimensional MHD simulations of Ganymede's magnetosphere. *Journal of Geophysical Research*, 113(A6), A06212. <https://doi.org/10.1029/2007ja012748>

Johnson, R. E. (1985). Polar frost formation on Ganymede. *Icarus*, 62(2), 344–347. [https://doi.org/10.1016/0019-1035\(85\)90130-7](https://doi.org/10.1016/0019-1035(85)90130-7)

Johnson, R. E., Carlson, R. W., Cooper, J. F., Paranicas, C., Moore, M. H., & Wong, M. C. (2004). Radiation effects on the surfaces of the Galilean satellites. In F. Bagenal, T. E. Dowling, & W. B. McKinnon (Eds.), *Jupiter: The planet, satellites, and magnetosphere* (pp. 485–512). Cambridge University Press.

Khurana, K. K., Pappalardo, R. T., Murphy, N., & Denk, T. (2007). The origin of Ganymede's polar caps. *Icarus*, 191(1), 193–202. <https://doi.org/10.1016/j.icarus.2007.04.022>

Kollmann, P., Clark, G. B., Paranicas, C., Mauk, B., Haggerty, D. K., Rymer, A. M., & Allegrini, F. (2022). Ganymede's radiation cavity and radiation belts. *Geophysical Research Letters*, 49, e2022GL098474. <https://doi.org/10.1029/2022GL098474>

Ligier, N., Paranicas, C., Carter, J., Poulet, F., Calvin, W., Nordheim, T., et al. (2019). Surface composition and properties of Ganymede: Updates from ground-based observations with the near-infrared imaging spectrometer SINFONI/VLT/ESO. *Icarus*, 333, 496–515. <https://doi.org/10.1016/j.icarus.2019.06.013>

Liuzzo, L., Poppe, A. R., Paranicas, C., Nenon, Q., Fatemi, S., & Simon, S. (2020). Variability in the energetic electron bombardment of Ganymede. *Journal of Geophysical Research: Space Physics*, 125(9), e2020JA028347. <https://doi.org/10.1029/2020ja028347>

Ma, Q., Li, W., Zhang, X., Shen, X., Daly, A., Bortnik, J., et al. (2021). Energetic electron distributions near the magnetic equator in the Jovian plasma sheet and outer radiation belt using Juno observations. *Geophysical Research Letters*, 48(24). <https://doi.org/10.1029/2021GL095833>

Marconi, M. L. (2007). A kinetic model of Ganymede's atmosphere. *Icarus*, 190(1), 155–174. <https://doi.org/10.1016/j.icarus.2007.02.016>

Mauk, B. H., Haggerty, D. K., Jaskulek, S. E., Schlemm, C. E., Brown, L. E., Cooper, S. A., et al. (2017). The Jupiter energetic particle detector instrument (JEDI) investigation for the Juno mission. *Space Science Reviews*, 213(1–4), 289–346. <https://doi.org/10.1007/s11214-013-0025-3>

Mauk, B. H., Haggerty, D. K., Paranicas, C., Clark, G., Kollmann, P., Rymer, A. M., et al. (2018). Diverse electron and ion acceleration characteristics observed over Jupiter's main aurora. *Geophysical Research Letters*, 45(3), 1277–1285. <https://doi.org/10.1002/2017gl076901>

Pappalardo, R., Collins, G. C., Head, J. W., III, Helfenstein, P., McCord, T. B., Moore, J. M., et al. (2004). Geology of Ganymede. In F. Bagenal, T. E. Dowling, & W. B. McKinnon (Eds.), *Jupiter: The planet, satellites, and magnetosphere* (pp. 363–396). Cambridge University Press.

Paranicas, C., Mitchell, D., Krimigis, S., Hamilton, D., Roussos, E., Krupp, N., et al. (2008). Sources and losses of energetic protons in Saturn's magnetosphere. *Icarus*, 197(2), 519–525. <https://doi.org/10.1016/j.icarus.2008.05.011>

Paranicas, C., Paterson, W. R., Cheng, A. F., Mauk, B. H., McEntire, R. W., Frank, L. A., & Williams, D. J. (1999). Energetic particle observations near Ganymede. *Journal of Geophysical Research*, 104(A8), 17459–17469. <https://doi.org/10.1029/1999ja900199>

Paranicas, C., Szalay, J. R., Mauk, B. H., Clark, G., Kollmann, P., Haggerty, D. K., et al. (2021). Energy spectra near Ganymede from Juno data. *Geophysical Research Letters*, 48(10). <https://doi.org/10.1029/2021GL093021>

Plainaki, C., Massetti, S., Jia, X., Mura, A., Milillo, A., Grassi, D., et al. (2020). Kinetic simulations of the Jovian energetic ion circulation around Ganymede. *The Astrophysical Journal*, 74(1). <https://doi.org/10.3847/1538-4357/aba94c>

Plainaki, C., Milillo, A., Massetti, S., Mura, A., Jia, X., Orsini, S., et al. (2015). The H₂O and O₂ exospheres of Ganymede: The result of a complex interaction between the Jovian magnetospheric ions and the icy moon. *Icarus*, 245, 306–309. <https://doi.org/10.1016/j.icarus.2014.09.018>

Roth, L., Ivchenko, N., Gladstone, G. R., Saur, J., Grodent, D., Bonfond, B., et al. (2021). A sublimated water atmosphere on Ganymede detected from Hubble Space Telescope observations. *Nature Astronomy*, 1–9(10), 1043–1051. <https://doi.org/10.1038/s41550-021-01426-9>

Sievekka, E. M., & Johnson, R. E. (1982). Thermal- and plasma-induced molecular redistribution on the icy satellites. *Icarus*, 51(3), 528–548. [https://doi.org/10.1016/0019-1035\(82\)90144-0](https://doi.org/10.1016/0019-1035(82)90144-0)

Teolis, B. D., Wyrick, D., Bouquet, A., Magee, B., & Waite, J. (2017). Plume and surface feature structure and compositional effects on Europa's global exosphere: Preliminary Europa mission predictions. *Icarus*, 284, 18–29. <https://doi.org/10.1016/j.icarus.2016.10.027>

Williams, D. J., Mauk, B., & McEntire, R. W. (1998). Properties of Ganymede's magnetosphere as revealed by energetic particle observations. *Journal of Geophysical Research*, 103(A8), 17523–17534. <https://doi.org/10.1029/98ja01370>